INVESTIGATION OF TURBO MACHINERY AND JET NOISE OF THE V2500 ENGINE DURING GROUND TESTS WITH AN A320 AIRCRAFT

Henri Siller, Alessandro Bassetti, and Stefan Funke

German Aerospace Center (DLR), Institute of Propulsion Technology,
Department of Engine Acoustics,
Müller-Breslau-Str. 8, 10623 Berlin, D–10623 Germany

ABSTRACT

The noise emission of a V2500 engine during ground operation was investigated with the A320 research aircraft ATRA of the German aerospace center DLR. Acoustic measurements with a microphone array parallel to the engine shaft axis were performed with the engines running at different speeds between idle and maximum continuous thrust. The main measurements took place in a noise-protection hangar, because optical measurements with laser devices were performed in parallel. In order to assess the impact of the room acoustics on the sound field, reference measurements were performed under free-field conditions, using the same microphone array set up on the ground. The array data were analysed using classical spectral methods and the SODIX (source directivity modelling in the cross-spectral matrix) method. SODIX fits equivalent source distributions, for different frequency bands and emission directions, to the measured cross-spectral matrices. The results show sources at the engine inlet, nozzle and along the jet. When the spectra and source distributions from the main measurements in the hangar are compared to the free-field data, the deviations are acceptable. This confirms that this type of noise protection hangar is a suitable environment to perform acoustic measurements of aircraft engines.

NOMENCLATURE

BOS background oriented schlieren
BPF blade passing frequency
EO engine order N1 engine primary shaft speed
PIV particle image velocimetry
SODIX Source directivity modelling in cross-spectral matrix

INTRODUCTION

The work presented in this paper was performed within the framework of the DLR project SAMURAI (Synergy of Advanced Measurement Techniques for Unsteady and High Reynolds Number Aerodynamic Investigations). In this project, several DLR institutes performed joint measurements to investigate the acoustic and aerodynamic characteristics of the V2500 engines of the A320 DLR research aircraft ATRA during static ground tests. The purpose of these tests was to demonstrate and test optical flow measurement techniques and acoustic analysis methods for future applications in large scale tests. Further objectives of the SAMURAI project have been to investigate the coupling of acoustic sources with structures in the turbulent flow and to validate complex and non-stationary numerical simulations of high Reynolds number jet flows. First results of the aerodynamic measurements have been reported by Schröder et al. (2014). The present paper presents results of the acoustic measurements and source localisation with linear microphone arrays. First results of the localisation analysis have already been presented in Siller et al. (2014) with a focus on the SODIX method. The present paper presents an improved analysis and presentation of the results. It also focusses on the turbomachinery noise aspects of the results.

The main experiments reported here were performed in September 2013 in the engine test hangar of Lufthansa Technik at Hamburg airport. This environment was not optimal for acoustic measurements, but had to be chosen in order to comply with laser safety regulations and to be independent of the weather conditions. In order to quantify the unknown impact of the reflections of acoustic waves from the roof and walls of the hangar, reference measurements were performed under free-field conditions at the airfield in Cochstedt in May 2013.

For the data reduction, standard spectral methods are used to analyse the directivity of the noise field and the SODIX (source directivity modelling in the cross-spectral matrix) method (Michel and Funke, 2008a,b,c; Funke et al., 2012b, 2014a) is used to analyse the sound field of the engine by calculating equivalent noise source distributions for different frequencies and emission directions. The Cochstedt and Hamburg results are compared in order to assess the impact of the partially reverberating environment in the Hamburg hangar on the acoustic data.

The expertise for acoustic tests of full-size turboshaft engines has been built up at the DLR engine acoustics group over a long time, starting with static acoustic outdoor tests with linear microphone arrays (Siller et al., 2001). From the experience with free-field tests, a method for indoor test-cells has been developed (Böhning et al., 2006; Funke et al., 2011, 2012a; Schnell et al., 2012; Funke et al., 2014b) and improved.

EXPERIMENTAL SET-UP

During both experiments, the DLR research aircraft ATRA was parked with the brakes on and the engines running. A linear microphone array was set up parallel to the axis of one engine and measured the sound field at different engine speeds that were kept constant during the data acquisition. For the free-field experiments in Cochstedt (CO), the aircraft was parked on the tarmac with no obstructions within a distance of several hundred meters. The Hamburg experiments took place in a noise protection hangar with indoor dimensions of 95 m length and a width of 78 m. The side walls and roof have acoustic linings, the inlet gate consists of an array of vertical acoustically lined flow guide vanes and the exit has a jet deflector rake and a noise barrier (Donges SteelTec GmbH, 2002).

Engines and engine speed

The engines of the ATRA are International Aero Engine (IAE) engines of the type V2527-A5 (see e.g. Airbus (2012) for more information). They are long cowl engines, where the hot core and the cold bypass flows mix inside the nacelle and exit through a common nozzle, which has an inner diameter of 1.067 m.

In both experiments, the array data were measured with both engines running at different engine shaft speeds between idle ($N1 = 30\%$) and maximum continuous thrust ($N1 = 82\%$). The aircraft was held in position by the brakes on the landing gear only. The movement of the aircraft due to the forward thrust, which occurred due to movements of the landing gear suspension systems, was monitored with a camera and remained below 20 cm at the highest engine speeds.

Microphone array and coordinate system

Figure 1 shows the set-ups of the array and the aircraft. The measurements were performed on the starboard side engine at Cochstedt and on the the port side engine in Hamburg. Originally, an identical set-up had been planned for both tests, but local conditions called for the aircraft to be turned for the main test.

This change implies a change in the coordinate system: for the Cochstedt data, the y-axis of the coordinate system points from the engine towards the array, for the Hamburg data in the opposite direction. The coordinate system was centred at the nozzle exit plane on the engine axis (see figure 2) with the x-axis pointing in the direction of the jet, the z-axis pointing upwards and the y-direction according to the convention of a right-handed coordinate system.

Acoustic data acquisiton

Both experiments were performed using the same equipment. The linear microphone array, a modular set-up with 248 microphones mounted on rail segments, was used to measure the sound field of the engine from a sideway distance of $10\,\mathrm{m}$. The array was 46.3 m long and the microphones were set with a constant spacing of $120\,\mathrm{mm}$ in the central section of the array, which is 13.3 m long. Towards both ends, the spacing gradually increased up to $577\,\mathrm{mm}$.

The array system was constructed such that the analogue signal path was kept relatively short and that the operating personnel could be as far away from the aircraft engines as possible. The analogue to digital conversion was performed in AD converter boxes situated relatively close to the microphones. In groups of eight, the microphones were connected to concentrator boxes via $10\,\mathrm{m}$ of analogue cable, which were connected to the 32 channel AD converters in groups of four. The eight AD converter boxes were connected with digital cables of $50\,\mathrm{m}$ length to the data acquisition unit which was controlled over an optical fibre link. In the free field experiment, sound pressure levels up to 100 dB were measured using a hand-held sound level meter at a distance of approximately $30\,\mathrm{m}$ away from the aircraft.

The procedure for the acoustic tests was to run the engine up to the desired speed. When the engine shaft speed had reached a stable level, data were acquired for a period of $40\,\mathrm{s}$ for all of the 248 array microphones simultaneously, at a sampling rate of $f_s = 40\,\mathrm{kHz}$.

DATA ANALYSIS AND RESULTS

Frequency spectra measured in the free field and the hangar

The two measurements performed under acoustic free-field conditions and in the partially reverberating environment of the hangar are first compared on the basis of frequency spectra. The spectra vary depending on their position due to the strong directivity of the sound sources of the engine and the jet. A suitable parameter for a comparison is the spatially averaged spectrum based on all array microphones. These spectra were calculated by first calculating time averaged frequency spectra from the measured time series of all array microphones and then averaging these spectra over all array microphone positions. For a better comparison and analysis of tonal components that are connected with the rotation frequency $N1$ of the primary shaft of the engine, the frequency is scaled to engine orders (EO) with the primary shaft frequency $N1$. Engine-order spectra are determined as narrow-band spectra, where the band width is proportional to the primary-shaft rotation frequency. In the present case, the frequency resolution is set to half an engine order in order to distinguish multiples of the shaft frequency from other frequency components.

The engine orders can also be presented as multiples of the blade passing frequency (BPF). In the engine order spectra, the blade passing tones can be found at engine orders with values that are multiples of the number of blades of a particular stage on the primary shaft. The most prominent tones are the BPF of the fan and its harmonics, which occur at engine orders of multiples of 22, the number of fan blades of the V2500 engine. When the frequency is scaled with the BPF, the fan tone harmonics occur at integer values of the BPF axis.

In figures 3a and 4, we report these type of spectra: In figure 3a, the frequencies are given in engine orders, while in figure 4, the frequency is scaled with the fan BPF.

Figure 3a shows spatially averaged spectra from the experiment in the Hamburg hangar for four different engine shaft speeds with $N1 = 30, 50, 72$, and $82\,\%$ (these data are from the second test run in Hamburg, HH2 in figure 3b). The frequency is scaled to engine orders so that tonal noise components that originate from a turbomachinery stage that is fixed to the primary shaft can be identified as spikes at integer values on the EO axis. Such tones remain at the same engine order when the engine speed changes and only change in amplitude. Figure 3a shows tones below the first BPF tone at engine speeds of $N1 = 30\%$ and $N1 = 50\%$, which are not generated by a mechanism that is linked to the low pressure shaft because they move up to higher engine orders when the shaft speed is increased.

Fan tones are visible in figure 3a at the fan BPF, at EO 22, and its higher harmonics, at EOs 44, 66, and 88. The fourth BPF at EO 88 is not very pronounced, but it is surrounded by two loud tones at $EO = 85$ and 89 which can be identified as the BPFs of the last two stages of the low-pressure turbine which have 85 and 89 blades. The turbine tones are dominant in the rear arc, see also figure 6, and they are surrounded by a typical hay-stack shape, that is caused by the scattering of the sound as it propagates through the turbulent shear layer of the exhaust jet.

The measurement uncertainty of the spectral data is remarkably low: two repeat measurements (not shown here) have maximum differences below 0.2 dB in the broadband noise between the engine tones. The tones themselves differed by as much as a couple of dB, which is more linked to the generation and propagation of the tones than to the measurement technique.

On a global level, the repeatability of the results is also very high: figure 3b presents the overall sound pressure level (OASPL) for the two repeat runs of the engine tests under free-field (CO) conditions and in the hangar (HH). The OASPL was calculated by integrating the frequency spectra in the range between $50\,\mathrm{Hz} \leq f \leq 15\,\mathrm{kHz}$. The repeat measurements coincide with each other and even the free-field and the indoor results differ by less than one dB.

Figure 4 presents a different view on the spatially averaged frequency spectra: the sound pressure level is shown as a contour plot the frequency as a function of the frequency scaled to multiples of the BPF on the vertical axis and the $N1$ shaft speed in percent along the horizontal axis. The sound pressure levels increase with the shaft speed, especially at low frequencies, where the jet noise dominates.

Figures 4a and 4b agree well qualitatively and with respect to the levels of the BPF tones and broad band noise. This is remarkable, considering that the experiments were performed under different conditions, with a period of four month in between and for different engines of the same aircraft.

The sound sources of an aircraft engine are highly directive. Frequency spectra measured with individual microphones at five positions situated at emission angles between $\theta = 150°$ in the forward arc and $\theta = 30°$ to the rear in steps of $30°$ are presented in figures 6. Two spectra are presented for two different engine speeds with $N1 = 60\,\%$ and $N1 = 82\,\%$ for the free-field and the indoor test. The emission angle θ is measured in jet coordinates between the engine axis and the connecting line between a microphone position and the nozzle exit position on the engine axis.

At $N1 = 60\,\%$, the spectra in the forward arc are dominated by tones at the BPF of the fan and its higher harmonics. The prominence of these tones is reduced towards the side line position. In the rear arc, the sound field is dominated by low frequency jet noise. At the maximum continuous thrust setting with $N1 = 82\,\%$, the fan tip speed is supersonic and multiple tone noise, or buzz-saw-noise, is radiated off the fan into the forward arc. At the side line position, the only remaining tones are the BPF harmonics and some interaction tones of minor importance. In the rear arc, the spectra are, again, dominated by low-frequency jet noise. The tonal noise is of course much higher than in flight or at static engine tests. Static engine tests are usually performed with a turbulence control screen over the engine intake that reduces the effect of inflow distortions like the ground vortex that is sucked into the inlet. The PIV measurements performed in the noise protection hangar and photographic evidence from the free-field test show a strong ground vortex in the lower region of the engine inlet.

The turbine tones that occur near the fourth BPF are, as one could expect, strongest in the rear arc. They appear in the side line direction at $\theta = 90°$ and increase in amplitude towards the rear arc, with a maximum at $\theta = 60°$.

As noted in the discussion of the engine order spectra, it is remarkable that the frequency spectra, which were measured at different times, locations, and even for the two different engines of the ATRA (the starboard side engine at Cochstedt, the port side in Hamburg), show a high degree of similarity. The tonal peaks are very sharp, which indicates the stability and accuracy of the engine speed settings which ensured an excellent repeatability of the results.

In the forward arc and to the side, the sound pressure levels measured indoors are significantly higher for frequencies below $300\,\text{Hz}$. This can be attributed to the low-frequency jet noise from both engines being reflected off the roof and side walls of the Hamburg hangar. In the rear arc, where the jet is the strongest source, the direct jet noise is strong enough to mask the impact of the reflections. In the forward arc, the distribution and strength of the buzz-saw noise peaks is different in both measurements. This not surprising because the flow conditions into the engine inlet were certainly different and also, because even engines of the same production type do have individual buzz saw noise signatures.

Source localisation with SODIX

The SODIX method is an inverse technique that reconstructs the measured sound field from a distribution of equivalent, incoherent, and directive point sources. Because the equivalent sources can have different amplitudes for every microphone position, the directivity of the sources is a result of the analysis.

SODIX was applied to the cross-spectral matrices from the Cochstedt and Hamburg experiments in order to localise the sound sources at the engine inlet, nozzle, and in the jet. The model source distributions were placed onto the engine axis. The length of the source region as well as the density of point sources on the line varied with the frequency. For one-third octave bands up to and including 250 Hz, the source region included 40 nozzle diameters downstream of the nozzle. For higher frequencies, the length reduced by a factor of two for a doubling of the frequency. The distance between the sources was set to $\Delta x = 0.25\,\lambda$, however some adjustments were made in the jet region downstream of the engine. Also, sources were placed directly at the positions of the engine intake and nozzle. SODIX performs the analysis for all narrow bands, but a different set of source positions was used for every one-third-octave band.

Figure 5 presents the SODIX results for the *maximum continuous thrust* condition, with an engine speed of $N1 = 82\%$. The high engine speed is a challenging case for any source localisation method. While the sound field is dominated by the jet noise, which radiates towards the rear arc, there are also strong tonal sources, which are generated by the *buzz-saw-noise* mechanism, that radiate out of the intake into the forward arc.

In figure 5, the source strengths are represented in a contour plot. The source positions are shown on the horizontal axis and the vertical axis represents the emission angle of each source. Along a vertical line in the plots, we see the directivity of a source at this particular position. The two vertical dashed lines mark the engine intake and nozzle positions.

In the lowest one-third-octave band shown, for $125\,\text{Hz}$ in figure 5, 89 sources were distributed along the engine axis. The results show a strong source at the nozzle and a separate extended source region in the jet, which both radiate downstream. In the hangar, the nozzle source is several dB louder than in the free field. The horizontal ripples in the plot for the indoor measurements for the microphones far downstream are caused by refraction at a column near the microphones in that region.

One octave higher, at $250\,\text{Hz}$ in figure 5, 176 sources have been calculated. There is source at the intake that radiates upstream, with a different directivity in the free field and in the hangar, and an extended source region in the jet.

At $500\,\text{Hz}$, see figure 5, the number of sources has been increased to 206. The inlet source is much weaker in the free-field than in the hangar, probably due to different inflow distortions for the fan and different *buzz-saw-noise* characteristics of the starboard and port side engines. This effect also shows up in the $500\,\text{Hz}$ one-third-octave band in figure 6, where two tones within this band have amplitudes that are several dB above the free-field measurements.

In the $f = 1\,\text{kHz}$ band, see figure 5, the x-axis length has been reduced to $-8 <= y <= 12\,\text{m}$ in order to limit the number of sources to be computed to 265. In this frequency band, there is a strong source at the engine inlet position that radiates into the forward direction. The inlet source has an interference pattern which is most likely the effect of the modal structure of the buzz tones in this band (see figure 6). The pattern is more pronounced in the free-field experiment, where the inflow distortions were probably lower. In the hangar, where the flow is probably distorted by the wakes of the inlet guide vanes of the noise protection hangar, the directivity of the tones averages out.

CONCLUSIONS

Acoustic measurements with a linear microphone array have been performed during ground tests of the DLR ATRA aircraft on an open airfield and inside a noise protection hangar. This set-up is different from that used for standard acoustic engine tests because of the proximity of the ground, but nevertheless very useful to investigate acoustic characteristics of an engine. The array data was used to analyse the frequency spectra at different emission angles and the SODIX algorithm was used in order to localise the directivity of the sound sources at the engine inlet, nozzle, and in the jet. The sound pressure levels measured in the free-field test were reproduced within a couple of dB difference in the noise protection hall. The broad band contribution was best reproduced apart from some differences that can be explained with reflection and refraction effects. Even the tonal levels, which depend on the inflow condition into the fan, could be reproduced within a few dB. This is remarkable because the tonal levels measured in engine test-cells normally exceed the free-field levels by over $10\,\text{dB}$ Funke et al. (2014b) due to the increased distortions of the flow onto the fan face. The frequency spectra of the free field and the hangar tests match very well apart from low-frequency effects due to reverberations in the hall.

An important noise contribution are the turbine tones of the V2500 engine. The turbine tones can be expected to have similar amplitudes in flight because they are generated at the end of the engine core, and are not modified by inflow distortions like the fan BPF tones. In flight, the haystacking effect that partially masks the turbine tones will also be reduced due to the smaller velocity difference across the jet, which will make the tones even more prominent.

The SODIX analysis reveals which sources are modified by the measuring environment and helps to interpret the frequency spectra. The source localisation with SODIX provides source amplitude maps that represent the source directivity of a particular source position along the engine axis. These source distributions can be used to calculate the frequency spectrum at a particular measurement point away from the engine. The SODIX analysis works well in both environments, apart from some deviations that can be explained with reverberation and refraction effects in the hangar.

ACKNOWLEDGEMENTS

The authors gratefully acknowledge the support by the staff of Lufthansa Technik at Hamburg Airport. During his internship at DLR, Simon Davies from the University of Cambridge did a great job in the initial preparation and analysis of the data.

ILLUSTRATIONS AND TABLES

(a)

(b)

Figure 1: Set-up of the linear microphone array: a) at the Cochstedt airfield and b) in the noise protection hangar of Lufthansa Technik at Hamburg airport (Images: DLR)

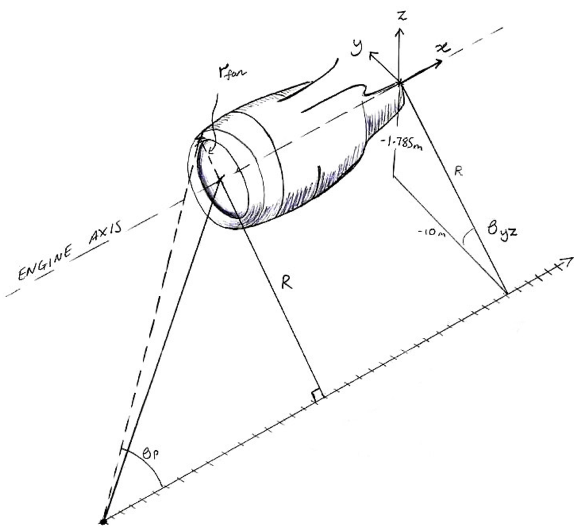

(a)

(b)

Figure 2: (a): Schematic of the set-up and definition of the coordinate system in the engine test hall of Lufthansa Technik at Hamburg airport (Image: Simon Davies, DLR). (b): the starboard side V2500 engine of the DLR ATRA (Image: DLR)

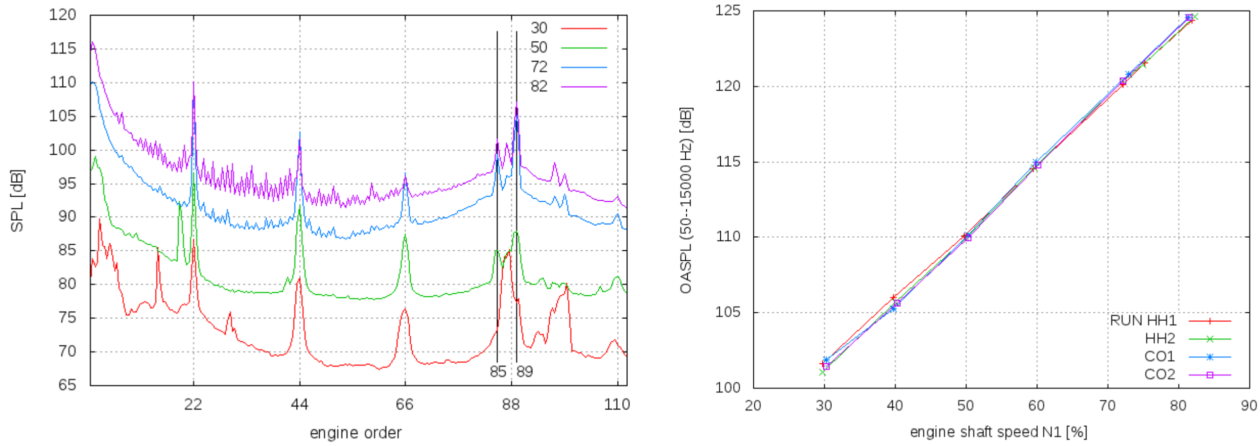

(a) (b)

Figure 3: Results averaged over all microphones in the array: a) narrow-band frequency spectra for engine speeds $30, 50, 72$, and $82\,\%N1$, the frequency axis is scaled to engine orders with the primary ($N1$) shaft frequency. b) Overall sound pressure level integrated over all frequency bands between $50\,\mathrm{Hz} < f < 10\,\mathrm{kHz}$ for different engine runs in the free-field and the hangar experiments.

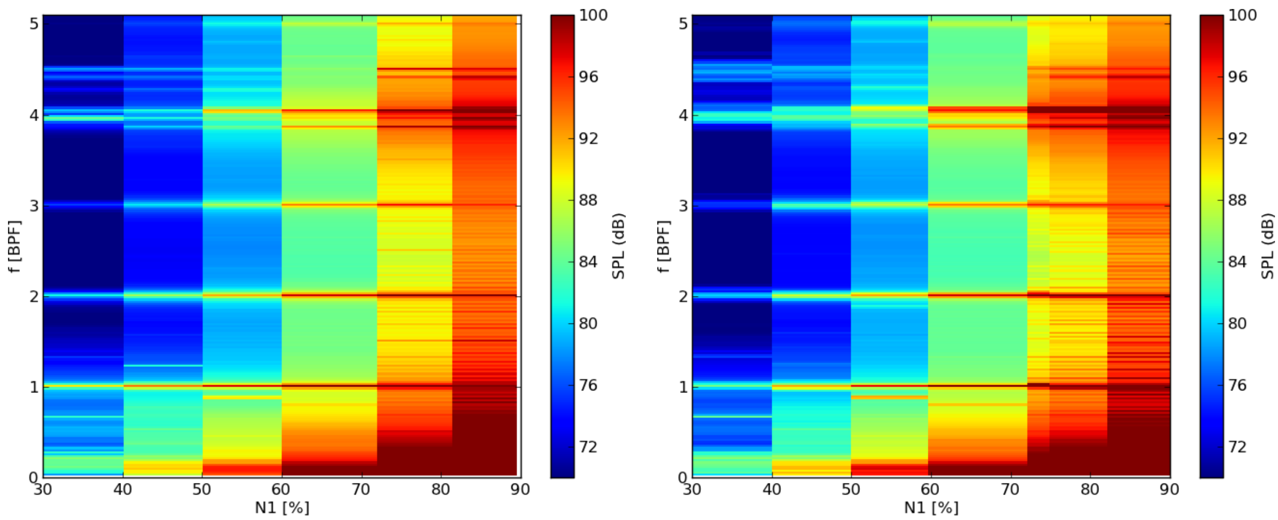

(a) (b)

Figure 4: Frequency spectra as a function of the $N1$ shaft speed: a) at the Cochstedt airfield and b) in the engine test hangar of Lufthansa Technik at Hamburg airport; data sets HH2 and CO2 from figure 3b were used for these plots.

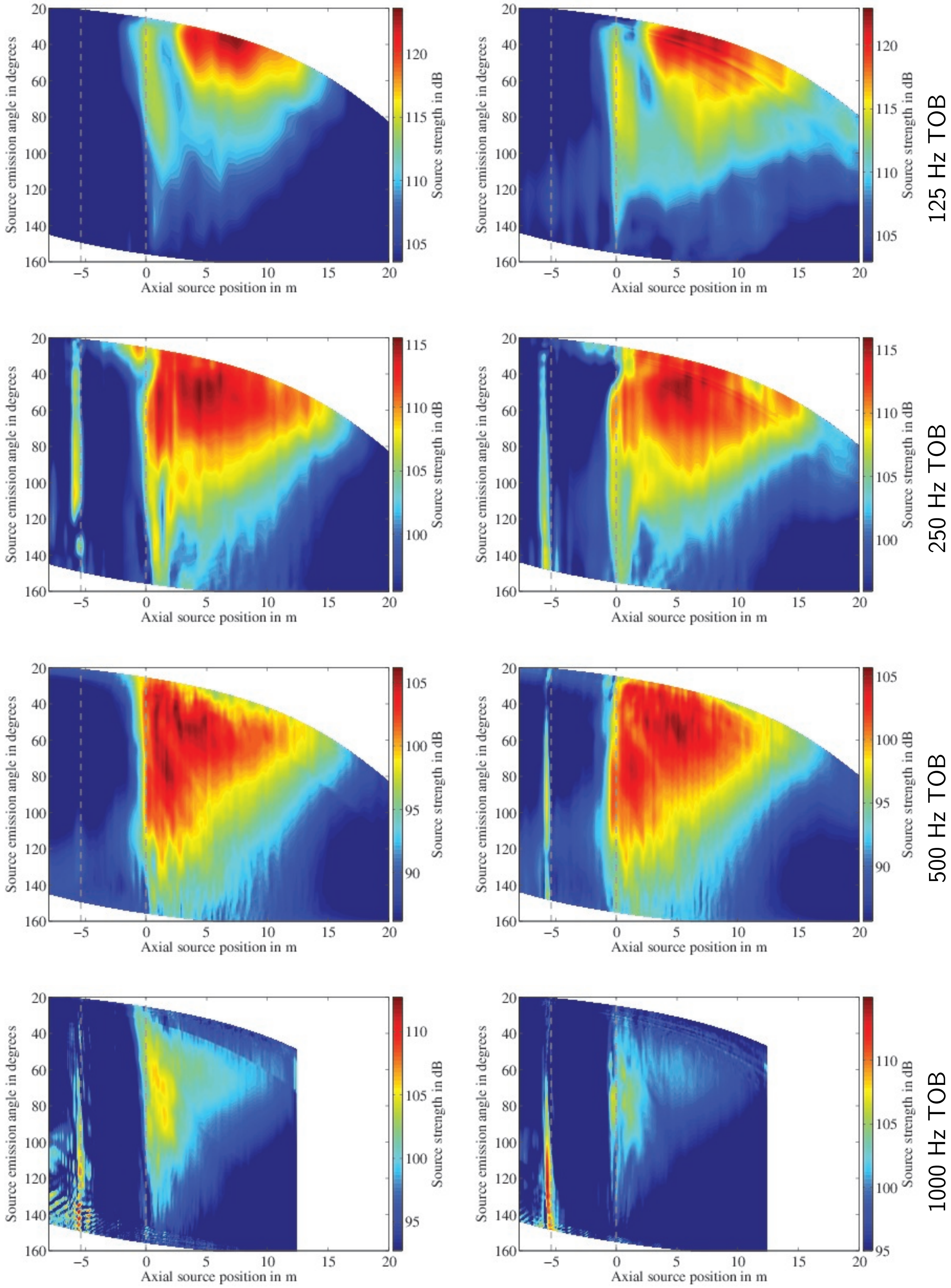

Figure 5: SODIX sound source directivity maps for the one-third-octave bands with 125 Hz, $250\,Hz$, 500 Hz, and 1 kHz. Left: Cochstedt , right: Hamburg experiment. The engine inlet (at $x = -5.2$ m) and nozzle positions (at $x = 0.0$ m) are marked with vertical dashed,, lines.

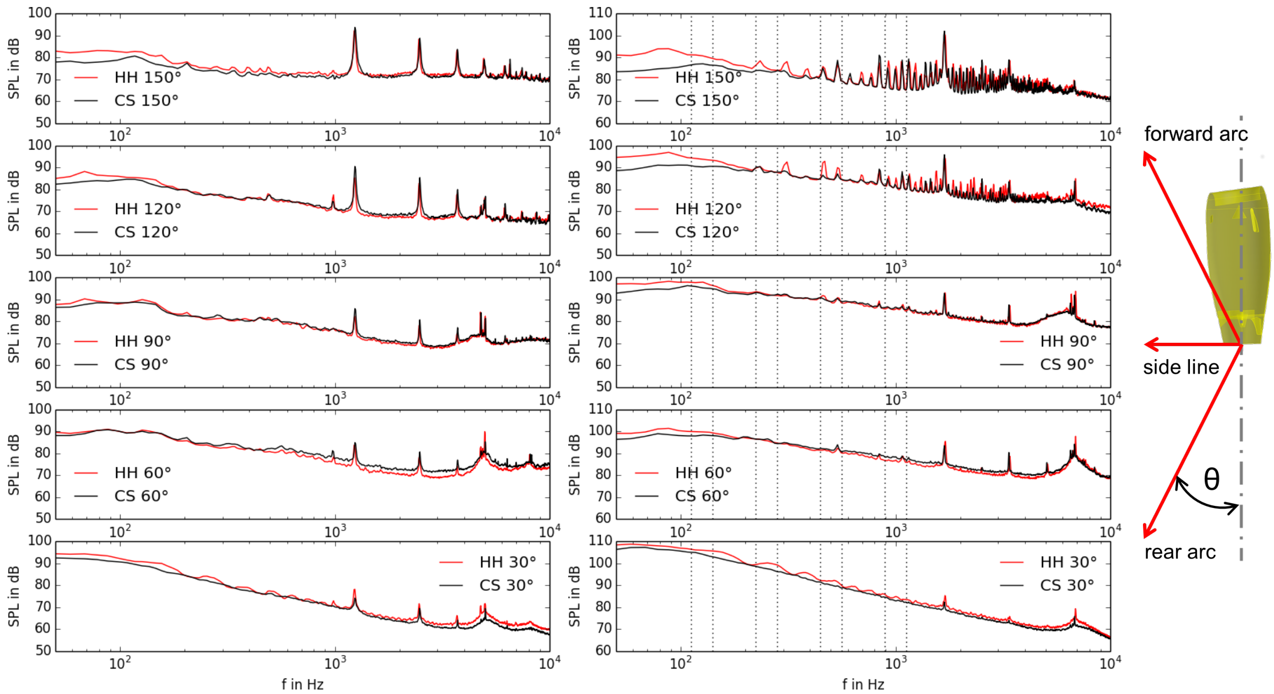

Figure 6: Frequency spectra for $N1 = 60\,\%$ (left) and $N1 = 82\,\%$ (right) measured under free-field (CS) and in-door conditions (HH) for different emission angles in jet coordinates between $150°$ in the forward arc and $30°$ in the rear arc. The vertical dotted lines in the plots for $N1 = 82\,\%$ mark the bounding frequencies of the 125 Hz, 250 Hz, 500 Hz and the 1 kHz one-third-octave bands.

References

Airbus. Airbus A320 aircraft characteristics airport and maintainance planning, 2012. Issue Sep 30/85, Rev: Jun 01/12.

P. Böhning, H. Siller, K. Holland, F. Arnold, A. Kempton, and U. Michel. Novel Methods for Acoustic Indoor Measurements and Applications in Aero-Engine Test Cells. 1st Berlin Beamforming Conference (BeBeC), November 22-23, 2006. Paper number BeBeC-2006-04.

Donges SteelTec GmbH. Noise protection halls for very large aircraft. Online document, 2002. URL `http://www.donges-steeltec.de/en/product-groups/air-traffic-structures/noise-protection-halls/noise-protection-halls-for-very-large-aircraft/`.

S. Funke, L. Kim, and H. Siller. Microphone-array measurements of a model scale contra-rotating open rotor in a reverberant open wind-tunnel. In *17th AIAA / CEAS Aeroacoustics Conference (32nd AIAA Aeroacoustics Conference)*. AIAA, 2011. URL `http://elib.dlr.de/74005/`.

S. Funke, L. Kim, and H. Siller. Acoustic measurements of a contra-rotating open rotor in an open jet wind-tunnel. *International Journal of Aeroacoustics*, 11(2):197–212, 2012a.

S. Funke, A. Skorpel, and U. Michel. An extended formulation of the SODIX method with application to aeroengine broad band noise. 18th AIAA/CEAS Aeroacoustics Conference, Colorado Springs, June 4-6, 2012b. Paper number AIAA-2012-2276.

S. Funke, R. P. Dougherty, and U. Michel. SODIX in comparison with various deconvolution methods. 5th Berlin Beamforming Conference (BeBeC), February 19-20, 2014a. URL `http://bebec.eu/`. Paper number BeBeC-2014-11.

S. Funke, H. Siller, W. Hage, and O. Lemke. Microphone-array measurements of a Rolls-Royce BR700 series aeroengine in an indoor test-bed and comparison with free-field data. In *20th AIAA/CEAS Aeroacoustics Conference, Atlanta, Georgia, USA*. AIAA, June 2014b.

U. Michel and S. Funke. Noise Source Analysis of an Aeroengine with a New Inverse Method SODIX. AIAA Paper 2008-2860, 2008a. 14th AIAA/CEAS Aeroacoustics Conference, Vancouver, BC, Canada, May 5-7, 2008.

U. Michel and S. Funke. Inverse method for the acoustic source analysis of an aeroengine. 2nd Berlin Beamforming Conference (BeBeC), February 19-20, 2008b. URL `http://bebec.eu/`. Paper number BeBeC-2008-12.

U. Michel and S. Funke. Noise Source Analysis of an Aeroengine with a New Inverse Method SODIX. AIAA-2008-2860, May 5-7, 2008c. 14th AIAA/CEAS Aeroacoustics Conference, Vancouver, BC, Canada.

R. Schnell, J. Yin, S. Funke, and H. Siller. Aerodynamic and basic acoustic optimization of a counter open rotor with experimental verification. In *AIAA Aeroacoustics Conference 2012*, Juni 2012. URL `http://elib.dlr.de/76253/`.

A. Schröder, R. Geisler, D. Schanz, J. Agocs, D. Pallek, M. Schroll, J. Klinner, M. Beversdorff, M. Voges, and C. Willert. Application of image based measurement techniques for the investigation of aeroengine performance on a commercial aircraft in ground operation, Juli 07-10 2014. 17th International Symposium on Applications of Laser Techniques to Fluid Mechanics Lisbon, Portugal.

H. Siller, A. Bassetti, S. Davies, and S. Funke. Investigation of the noise emission of the V2500 engine of an A320 aircraft during ground tests with a line array and SODIX. In *Proceedings on CD of the 5th Berlin Beamforming Conference, 19-20 February 2014*. GFaI, Gesellschaft zu Förderung angewandter Informatik e.V., Berlin, 2014. URL `http://bebec.eu/Downloads/BeBeC2014/Papers/BeBeC-2014-18.pdf`.

H. A. Siller, F. Arnold, and U. Michel. Investigation of aero-engine core-noise using a phased microphone array. AIAA paper 2001-2269, 2001. 7th AIAA/CEAS Aeroacoustics Conference and Exhibit, Maastricht, Netherlands, May 28-30, 2001, Collection of Technical Papers. Vol. 2 (A01-30800 07-71).